Hindawi
Shock and Vibration
Volume 2018, Article ID 7458529, 9 pages
https://doi.org/10.1155/2018/7458529

Research Article

Numerical Study on Aerostatic Instability Modes of the Double-Main-Span Suspension Bridge

Qiang Zhou,[1] Haili Liao,[1] and Tong Wang[2]

[1]*Research Center for Wind Engineering, Southwest Jiaotong University, Chengdu, China*
[2]*College of Civil Engineering, Shanghai Normal University, Shanghai, China*

Correspondence should be addressed to Tong Wang; tongwang@shnu.edu.cn

Received 20 September 2017; Revised 21 November 2017; Accepted 20 December 2017; Published 28 January 2018

Academic Editor: Chao Tao

In order to investigate the aerostatic instability mode and underlying failure mechanism of the new suspension bridge with double main spans, a corresponding program based on aerostatic load increment and two-iteration scheme was developed with considering the effects of aerostatic and geometric nonlinearity. Three double-main-span suspension bridges were taken as a case study to analyze the full range of aerostatic instability with different initial attack angles. Results show that there are two aerostatic instability modes for the double-main-span suspension bridge, one of which is the bilateral antisymmetric instability mode and the other is the single-span instability mode. The critical aerostatic velocity corresponds to the instability mode that occurs first, which is dependent on structural dynamic properties and initial attack angles. In addition, mechanism of the two aerostatic instability modes was discussed in detail.

1. Introduction

The single-span suspension bridge has been reported to be limited in the design of total length, which is up to 2~3 km [1]. For example, the latest record is Akashi Kaikyo Bridge with a central span of 1991 m. It could not meet the requirement for crossing straits and rivers nowadays, such as Yangtze River in China, Messina Strait in Italy, Tsugaru Strait in Japan, and Gibraltar Strait linking European and African Continents [2]. Alternatively, the suspension bridge with two or more main spans, which is one of the most favourable and economical solutions for wide and deep straits with longer span, comes into existence.

Currently, the existing practice in double or multispan suspension bridges includes the Chateauneuf Bridge with three main spans of 59.50 m, the Chatillon Bridge with double main spans of 76 m in France, the Konaruto Bridge with double main spans of 160 m in Japan, and the Save River Bridge with double main spans of 230 m in Mozambique. China has launched three double-long-span suspension bridges across the Yangtze River: Ma'anshan Yangtze River Bridge (MYB), Taizhou Yangtze River Bridge (TYB), and Wuhan Yingwuzhou Yangtze River Bridge (WYB). As shown in Figure 1, the span arrangements of MYB, TYB, and WYB are $360 + 2 \times 1080 + 360$ m, $390 + 2 \times 1080 + 390$ m, and $25 + 2 \times 850 + 225$ m, respectively.

For the long-span suspension bridge with double main spans, one of the most important wind-induced issues is the aerostatic instability, which may have an aerodynamic disadvantage of aerostatic instability compared to single-long-span suspension bridges [3]. Hirai et al. [4] observed the wind-induced lateral-torsional buckling phenomenon in wind tunnel tests of a full bridge aeroelastic model for a suspension bridge and suggested that the aerostatic instability of long-span bridges could occur under the action of static wind loads. Thereafter, some researchers [5–8] also found that the aerostatic instability of long-span bridges might occur before the dynamic instability and developed numerical methods to confirm the aerostatic instability. Boonyapinyo et al. [5] applied a nonlinear method, which combined the effects of the nonlinear three-component displacement-dependent wind loads and geometric nonlinearity, to investigate the wind-induced nonlinear lateral-torsional buckling of cable-stayed bridges. Cheng et al. [9] proposed a nonlinear method

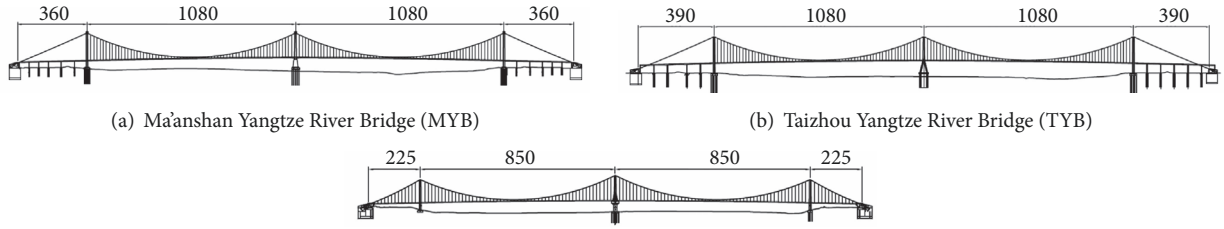

(a) Ma'anshan Yangtze River Bridge (MYB)

(b) Taizhou Yangtze River Bridge (TYB)

(c) Wuhan Yingwuzhou Yangtze River Bridge (WYB)

Figure 1: The configuration of three suspension bridges.

based on the one-incremental and two-iterative solution scheme for aerostatic instability problems of long-span suspension bridges and found that the aerostatic instability of the structure occurs when the deformed structure cannot resist the wind force and inversely enlarges the displacement-dependent tricomponent wind loads. Thereafter, this method has been widely used to analyze the aerostatic instability problem of long-span bridges [3, 10, 11]. Zhang and Yao [12] conducted a numerical investigation on the wind-induced deformation of super long-span cable-stayed bridges and discussed their aerostatic stabilities. These studies showed that the incorporation of the tricomponent displacement-dependent wind loads and the geometric nonlinearity in the analysis resulted in a significant reduction in the critical wind velocity for aerostatic instability [11].

However, most of the above researches were focused on the aerostatic stability analysis of cable-stayed bridges with a single main span. It is essential to consider the aerostatic stability for a suspension bridge with double main spans. In this paper, considering the effects of geometric nonlinearity and the aerostatic load nonlinearity, a procedure based on wind speed increment and two-iteration scheme was programmed and applied to analyze the aerostatic stability of three double-main-span suspension bridges (MYB, TYB, and WYB). The aerostatic instability mode and the underlying failure mechanism were discussed in detail.

2. Analytical Method

The aerostatic instability problem of long-span suspension bridges is the combination of the nonlinear aerostatic load behaviour and nonlinear bridge response [3]. The nonlinear aerostatic load is induced by the tricomponent wind load which is dependent on the displacement of the deck, as well as the initial attack angle. Furthermore, as the structural characteristic of the suspension bridge with double main spans is expressed as geometrical nonlinearity, thus it is a double nonlinearity during the analysis of the aerostatic instability problem.

2.1. Aerostatic Load. The three components of static wind load are drag force (in the along-wind direction), lift force (in the cross-wind direction), and pitch moment (in the clockwise direction). Considering a two-dimensional cross section of bridge deck in a smooth flow, as shown in Figure 2,

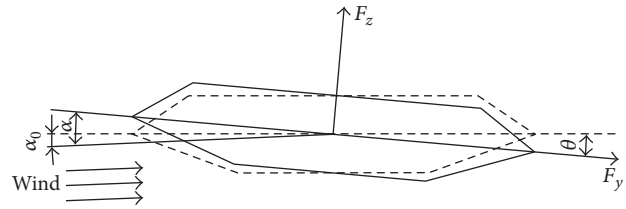

Figure 2: Three components of aerostatic load.

the three components of aerodynamic forces per unit span acting on the deformed deck can be expressed as follows:

$$F_y = \frac{1}{2}\rho U^2 C_y(\alpha) H,$$
$$F_z = \frac{1}{2}\rho U^2 C_z(\alpha) B, \quad (1)$$
$$F_M = \frac{1}{2}\rho U^2 C_M(\alpha) B^2,$$

where F_y, F_z, and F_M are drag force, lift force, and pitch moment, respectively; ρ is the air density; U is the wind velocity; $C_y(\alpha)$, $C_z(\alpha)$, and $C_M(\alpha)$ are the coefficients of drag force, lift force, and pitch moment in wind axes, respectively; α is the effective attack angle of wind which is the sum of initial attack angle α_0 and the torsional displacement of the deck θ; B is the deck width; H is the vertical projected area of the deck. Figure 2 shows the three components of static wind load of bridge deck.

2.2. Aerostatic Instability Analysis Method. The wind loads in (1) are the function of the torsional displacement of the girder, and the nonlinear equilibrium equation under wind load can be expressed as

$$[K(u)] \bullet \{u\} = P\left(F_Y(\alpha), F_Z(\alpha), F_M(\alpha)\right), \quad (2)$$

where $K(u)$ is the structural stiffness matrix including elastic stiffness matrix and geometrical stiffness matrix; $\{u\}$ is the displacement vector. The geometric nonlinearities of a cable-stayed bridge originate from three primary sources: cable sag effect, combined axial load and bending moment interaction for the elements, and large displacement, which are produced by the geometry changes of the structure [13]. Then, the

procedure of aerostatic instability analysis is presented as follows:

(a) Assume an initial wind attack angle α_0, an initial wind speed U_0, an increment of wind speed ΔU, the maximum number of internal iteration steps $N_{\max}$, and the maximum number of external iteration steps $M_{\max}$.

(b) Set the current wind speed as the initial wind speed U_0.

(c) Calculate the wind loads on the bridge (F_Y, F_Z, and F_M) using the current wind speed U with the initial wind attack angle α_0.

(d) Solve equation (2) using the Newton-Raphson method to obtain the displacement.

(e) Obtain the torsional angle of bridge deck elements θ and calculate the effective angle of attack α.

(f) Check whether the Euclidean norm (see (3)) of the tricomponent force coefficients is less than the allowable value (here, it is taken as $\varepsilon_K = 0.002$):

$$\text{Norm}_k = \left\{ \frac{\sum_{i=1}^{N_e} \left[C_k\left(\alpha_j\right) - C_k\left(\alpha_{j-1}\right) \right]^2}{\sum_{i=1}^{N} \left[C_k\left(\alpha_j\right) \right]^2} \right\} \le \varepsilon_K, \quad k = Y, Z, M, \tag{3}$$

where N_e is the number of elements subjected to the displacement-dependent wind load.

(g) If (f) is satisfied, increase wind speed by ΔU, $U_{j+1} = U_j + \Delta U$, and go back to step (c).

(h) If (f) is not satisfied, check whether or not the number of internal iterations n is less than the maximum number $N_{\max}$. If $n < N_{\max}$, go back to step (d). If $n \ge N_{\max}$, reduce the increment of wind speed in half, $\Delta U = \Delta U/2$, and go back to step (b).

(i) Keep the iteration of steps (b) to (h) until the number of external steps is no less than the maximum number of external iteration steps. The current wind velocity is taken as the critical wind velocity.

Based on the procedure, the flow chart is presented in Figure 3 and the program is developed.

In order to validate the present nonlinear calculation method, the critical velocities of aerostatic instability on the other two cable-stayed bridges (MYB Bridge: a suspension bridge with double main spans; Sutong Bridge: an inclined cable-stayed bridge with a single main span of 1088 m) are compared with those of previous studies. As shown in Table 1, the critical aerostatic velocity obtained by the present method exhibits good agreement with previous results [14, 15]. This illustrates that the present nonlinear calculation method is suitable for analysis of the aerostatic instability of long-span cable-stayed bridges.

3. Results and Discussions

3.1. Aerodynamic Coefficients of the Deck. To investigate the tricomponent wind load coefficients of the three bridge decks, section model tests were carried out in a wind tunnel under uniform flow. The curves of drag, lift, and pitch moment coefficients with respect to wind angles of attack in a range from −12° to 12° are shown in Figure 4. It can be seen that the three bridge deck sections show a similar tendency in the variation of aerodynamic coefficients with the wind angle of attack. The drag coefficient reaches its minimum value near 0°, while getting higher when facing a larger angle of attack. The lift coefficient is negative when $\alpha = -12^\circ$ and increases with the angle of attack. When $\alpha > 5^\circ$, it begins to be positive. The pitch moment coefficient varies little when the angle of attack increases slightly from negative values to positive values. In addition, the drag forces on the towers, as well as on the cables and links, are taken into account.

3.2. Structural Dynamic Properties. A modal analysis is carried out for the three bridge models by 3D-FEM, as shown in Figure 5, to obtain the structural dynamic properties including natural frequencies and mode shapes descriptions as shown in Figure 6. Here, S and A represent symmetry and antisymmetry, respectively, while V and T represent vertical bending mode and torsional mode, respectively. It can be found that MYB and TYB have similar torsional modes with one torsional twist for each main span due to the similar structure arrangement where the girder is continuous through the middle tower. However, the girder of WYB twists clockwise and counterclockwise in each main span because the girders of each span are independent.

In addition, it can be found obviously that the frequency of antisymmetric modes (including the vertical and torsional mode) is smaller than that of the symmetric mode for all the three suspension bridges with double main spans. This suggests that the antisymmetric mode may occur easier than the symmetric mode.

3.3. Aerostatic Instability Mode. Lateral bending modes are insignificant when compared with vertical bending modes and torsional vibrating modes since the lateral bending natural frequencies are much larger (see Section 3.2). Herein, only vertical and torsional displacements are considered in determining aerostatic instability.

Figure 7 presents torsional and vertical displacements at midspan and quarter-span points for MYB and TYB with the wind speed in the conditions of initial attack angle of 0°, where L represents the left side, R represents the right side, M represents the middle-span point, and Q represents the quarter point. As shown in the figure, it can be found that torsional and vertical displacements on the left and the right side are approximately antisymmetrical to the current balanced position. Thus, this kind of aerostatic instability mode is defined here as "bilateral antisymmetric instability mode." In addition, it can be found that the critical aerostatic stable wind velocities for MYB and TYB with the initial attack angle of 0° are 122.5 m/s and 99 m/s, respectively.

However, the torsional and vertical displacements on two sides of MYB and TYB are no longer approximately antisymmetrical as shown in Figure 8, where the initial attack angle changes to +3°. The critical wind speeds for aerostatic instability of MYB and TYB with the initial attack angle of +3° are 140 m/s and 112.5 m/s, respectively. Similarly, the aerostatic instability shapes of WYB with the initial attack angles of 0° and +3° show dominant unstableness on one main

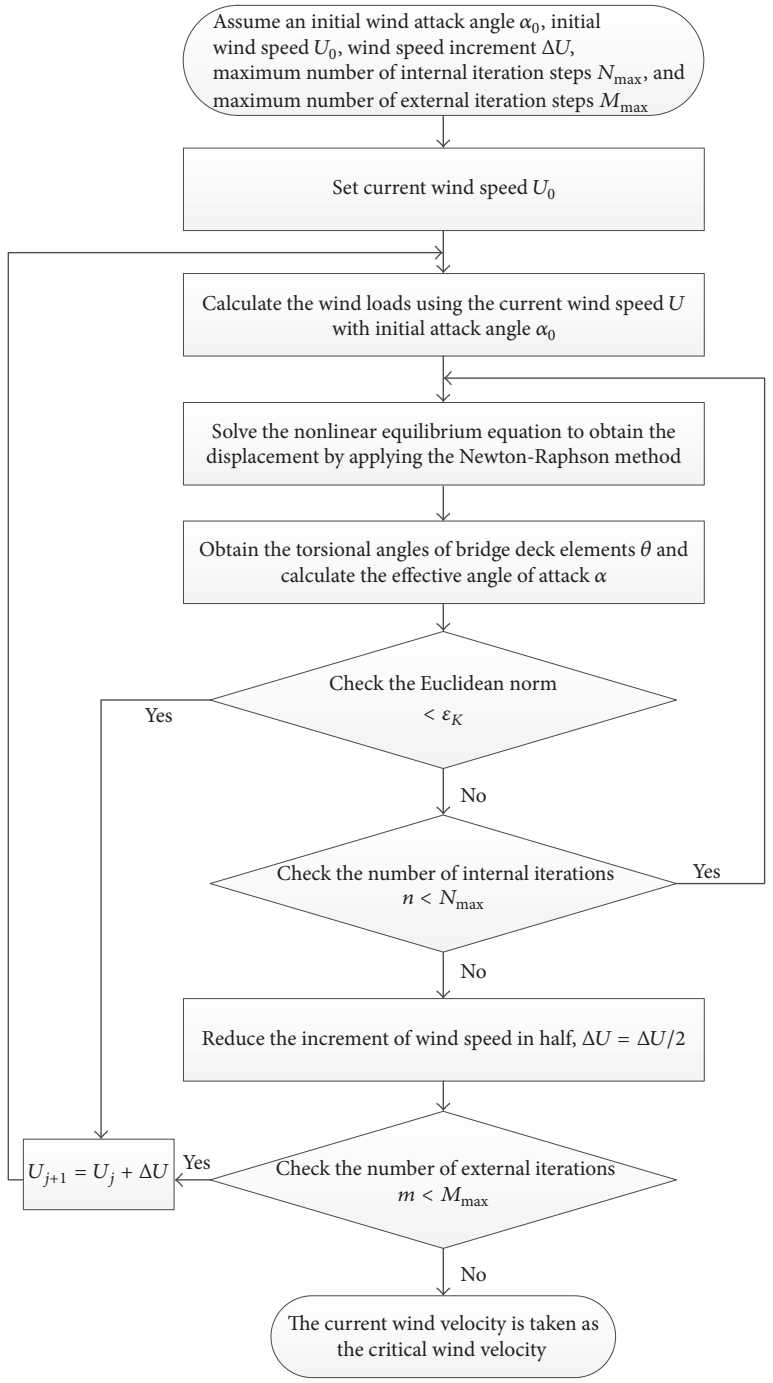

Figure 3: The flow chart of the procedure of aerostatic instability analysis method.

Table 1: Comparison of critical aerostatic velocity ($m \cdot s^{-1}$).

MYB Bridge	Present	Reference result [14]
	122.5	122
Sutong Bridge	Present	Reference result [15]
	99	96

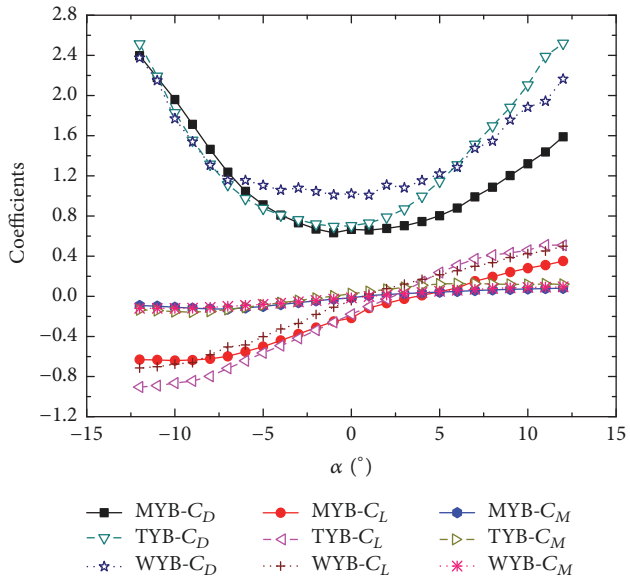

Figure 4: The aerodynamic coefficients of three bridge decks.

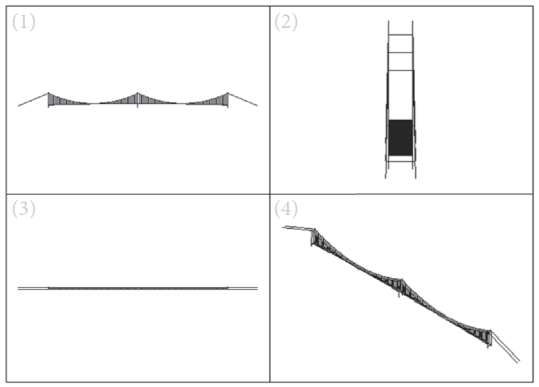

Figure 5: The 3D-FEM model of MYB.

span, and no approximately antisymmetrical or symmetrical form occurs as shown in Figure 9. This kind of aerostatic instability mode is defined here as "single-span instability mode."

As mentioned above, there are two kinds of aerostatic instability modes for suspension bridges with double main spans, one of which is antisymmetric instability mode and the other is single-span instability mode. Generally, the lift and moment coefficients of box-girder are positive with an attack angle of +3° as shown in Figure 4. Thus, the critical wind speed for aerostatic instability for an initial attack angle of +3° is less than that for an initial attack angle of 0°. However, comparing these two aerostatic instability modes of MYB and TYB as shown in Figures 7 and 8, it can be found that the critical wind speed for aerostatic instability with an initial attack angle of +3° is larger than that with an initial attack angle of 0°. In other words, the critical wind speed for bilateral antisymmetric instability mode is lower than that for single-span instability mode.

3.4. Failure Mechanism of Aerostatic Instability Mode. The process of aerostatic instability of structure is actually an interaction between the aerostatic loads and the structural stiffness. On the other hand, the structural stiffness, corresponding to one unique vibration mode, is related to the natural frequency of that vibration mode. Thus, the aerostatic instability of a bridge is associated with its structural dynamic properties. A similar point of view was also presented in previous researches [3, 10]. As shown in Figure 6, the symmetrical modes of double-main-span suspension occur later than the antisymmetrical modes according to their structural dynamic properties. Thus, it is more possible for the double-main-span suspension bridge that the mode of aerostatic instability would appear in an antisymmetrical form rather than a symmetrical form, or the aerostatic instability of one main span may occur. In addition, the different aerostatic instability modes may occur due to different initial wind attack angles.

3.4.1. Mechanism Analysis of Bilateral Antisymmetrical Instability Mode. Figures 10 and 11 present the aerostatic instability forms of MYB and TYB under an initial attack angle of 0°, which are the bilateral antisymmetrical instability mode as discussed in Section 3.3. It can be found that the bilateral antisymmetrical instability mode can be approximately expressed as the coupling deformation of the form of primary antisymmetrical vertical bending (A-V-1) and primary antisymmetrical torsion (A-T-1) modes, which are similar to the results of [3].

As shown in Figure 4, the lift coefficient of girder section is negative with an attack angle of 0°. This means the action direction of lift force is downward, which would increase the structural stiffness (including structural stiffness of single side main span). Thus, it is difficult for the single-span instability to occur. As for the suspension bridge with double spans, one of the most obvious characteristics is that the middle tower and the main cable provide the coordination. Therefore, when static wind loads increase to a certain value, which is larger than the resistance ability of one span, the displacement of this side span is quickly increased. Meanwhile, it will cause reverse displacement on another span with the coordination of the middle tower and main cable. Then, an approximate antisymmetric form happened. In addition, the frequencies of A-V-1 mode and A-T-1 mode are lower than that of the symmetrical mode. Moreover, according to the research of Arena et al. [16], the frequencies of A-V-1 mode and A-T-1 mode of long-span bridge would decrease much more with wind velocity than that of symmetrical mode. Therefore, from the energy point of view, the instability mode of suspension bridge with double main spans would occur with an antisymmetric form.

3.4.2. Mechanism Analysis of Single-Span Instability Mode. As shown in Figure 4, the lift coefficient of girder section is positive with an initial attack angle of +3°, which would result in an upward lift force. Therefore, the structural stiffness (including structural stiffness of single side main span) is weakened. With the increase of the effective attack angle between the structure and wind due to static wind loads,

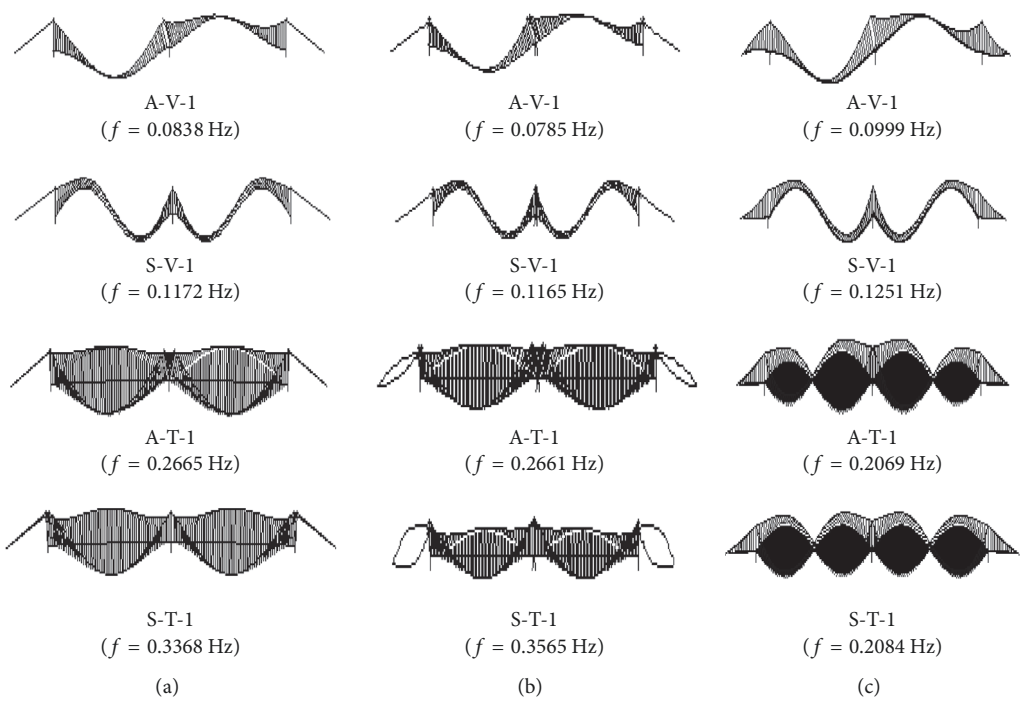

Figure 6: The primary structural dynamic properties of three bridges.

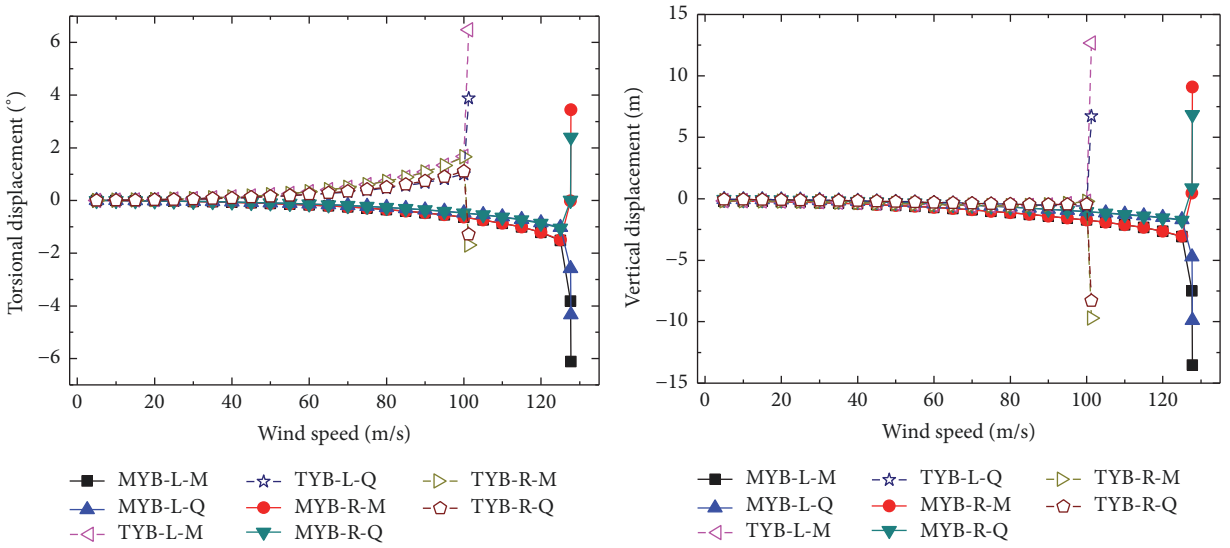

Figure 7: The torsional and vertical displacements for MYB and TYB with an initial attack angle of 0°. L: left; R: right; M: midspan point; Q: quarter-span point.

the synergies of the middle tower and main cables become weaker. In this situation, the aerostatic instability will firstly occur in one main span. In other words, the single-span instability mode form happened. In addition, the critical wind speed for aerostatic instability of one main span will increase due to fewer synergies of the middle tower.

In order to illustrate the single-span instability mode in detail, we compared the critical wind speed for aerostatic instability of single-span instability mode in TYB with that of Jiangyin Yangtze Bridge (JYB) with a single main span, which is similar to the length of one main span of TYB as shown in Table 2. It can be found that the critical wind speed for aerostatic instability of TYB is smaller than that of JYB as in the condition of attack angle of 0°. The reason is that the instability mode of TYB is the bilateral antisymmetrical instability mode, while JYB has the instability on its single

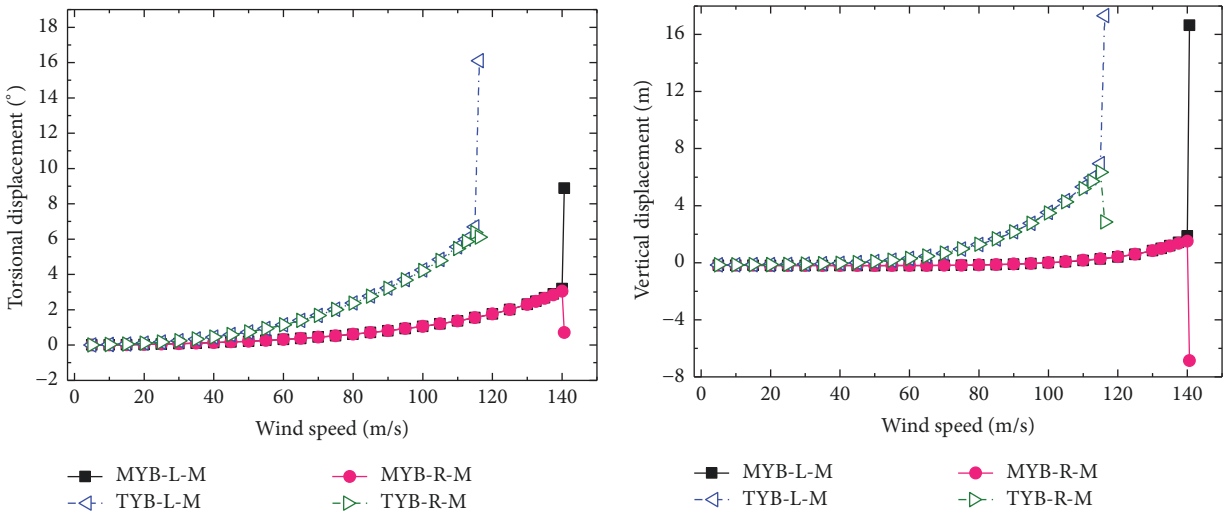

Figure 8: The torsional and vertical displacements for MYB and TYB with initial attack angles of +3°. L: left; R: right; M: midspan point.

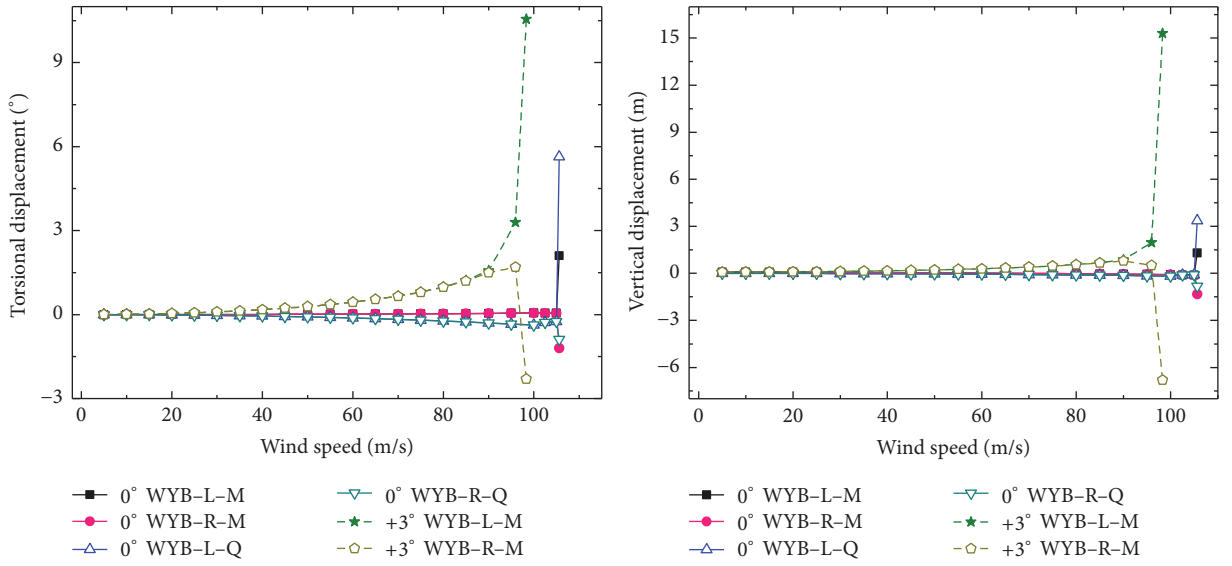

Figure 9: The torsional and vertical displacements for WYB with initial attack angles of 0° and +3°. L: left; R: right; M: midspan point; Q: quarter-span point.

main span. However, as for the cases of attack angle of +3°, the critical aerostatic stable wind velocities of TYB and JYB are similar to each other. This illustrates that the mechanism of single-span instability mode in the suspension bridge with double main spans is similar to that of a suspension bridge with single main span.

As for the case of WYB, its dynamic characteristic is quite different from those of MYB and TYB, due to the fact that the girders of each span are independent. As shown in Figure 6, the bridge twists clockwise and counterclockwise in each main span under the action of the wind load, which offset the imbalance of the two main spans, and the synergies of the middle tower and main cables become weaker. Thus, the single-span instability mode would occur much more easily in the case of WYB as shown in Figure 12.

4. Conclusions

Considering the effects of aerostatic and geometric nonlinearity, a nonlinear program was developed to analyze the aerostatic stability of three double-long-span suspension bridges: Ma'anshan Yangtze River Bridge (MYB), Taizhou Yangtze River Bridge (TYB), and Wuhan Yingwuzhou Yangtze River Bridge (WYB). The critical wind speed for aerostatic instability and the aerostatic instability modes as well as their mechanism are analyzed. Conclusions are summarized as follows:

(i) There are two aerostatic instability modes for double-main-span suspension bridges, one of which is the bilateral antisymmetric instability mode and the other is the single-span instability mode.

Table 2: The critical wind speed for aerostatic instability with different initial attack angles ($m \cdot s^{-1}$).

Name	Main span (m)	Initial attack angle	Critical wind speed*
TYB	2×1080	0°	99
		+3°	116
JYB	1385	0°	113
		+3°	110

*The results of JYB are from the literature of Cheng et al. [13].

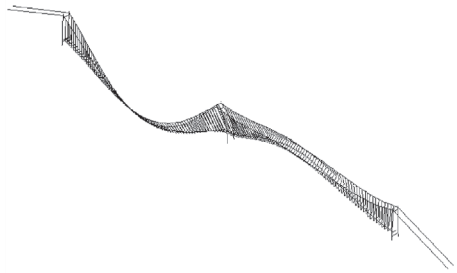

Figure 10: Aerostatic instability form of MYB under an initial attack angle of 0°.

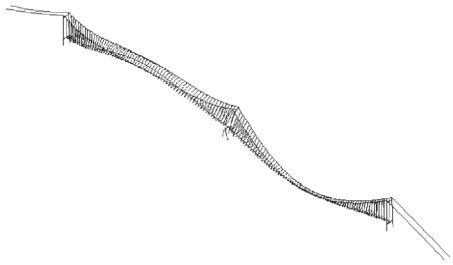

Figure 11: Aerostatic instability form of TYB under an initial attack angle of 0°.

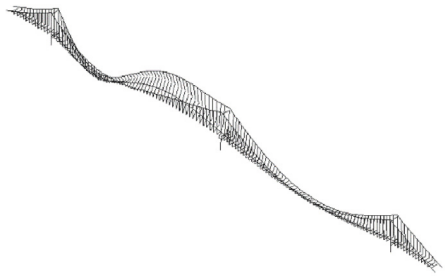

Figure 12: Aerostatic instability form of WYB under an initial attack angle of 0°.

(ii) The critical wind speed for aerostatic instability corresponds to the instability mode that emerges first, which is dependent on structural dynamic properties and initial wind angle of attack.

(iii) In the initial attack angle of 0°, as for the double-main-span suspension bridge with continuous deck crossing the middle tower, the aerostatic instability mode would be a bilateral antisymmetrical instability mode and the corresponding critical wind speed for aerostatic instability becomes lower.

(iv) The single-span instability mode of the double-main-span suspension bridge is similar to that of the single-span suspension bridge, and the corresponding critical wind speed for aerostatic instability is also similar.

Conflicts of Interest

The authors declare that they have no conflicts of interest.

Acknowledgments

This research was funded by the National Natural Science Foundation of China (Grants nos. 51378442, 51708462, and 51508333), the Fundamental Research Funds for the Central Universities (no. 2682016CX006), and Chongqing Basic and Frontier Research Project (cstc2014jcyjA30009).

References

[1] T. Forsberg, "Multi-span suspension bridges," *International Journal of Steel Structures*, vol. 1, pp. 63–73, 2001.

[2] Y. J. Ge and H. F. Xiang, "Extension of bridging capacity of cable-supported bridges using double main spans or twin parallel decks solutions," *Structure and Infrastructure Engineering*, vol. 7, no. 7-8, pp. 551–567, 2011.

[3] W. M. Zhang, Y. J. Ge, and M. L. Levitan, "Nonlinear aerostatic stability analysis of new suspension bridges with multiple main spans," *Journal of the Brazilian Society of Mechanical Sciences & Engineering*, vol. 35, no. 2, pp. 143–151, 2013.

[4] A. Hirai, I. Okauchi, M. Ito, and T. Miyata, "Studies on the critical wind velocity for suspension bridges," in *Proceedings of the International Research Seminar on Wind Effects on Buildings and Structures*, pp. 81–103, University of Toronto Press, Ontario, Canada, 1967.

[5] V. Boonyapinyo, Y. Lauhatanon, and P. Lukkunaprasit, "Nonlinear aerostatic stability analysis of suspension bridges," *Engineering Structures*, vol. 28, no. 5, pp. 793–803, 2006.

[6] V. Boonyapinyo, H. Yamada, and T. Miyata, "Wind-induced nonlinear lateral-torsional buckling of cable-stayed bridges," *Journal of Structural Engineering (United States)*, vol. 120, no. 2, pp. 486–506, 1994.

[7] M. Nagai, H. Yamaguchi, K. Nogami, and Y. Fujino, "Effect of cable size on static and dynamic instabilities of long-span cable-stayed bridges," *IABSE Symposium Report*, vol. 84, no. 7, pp. 33–40, 2001.

[8] X. Zhang, H. Xiang, and B. Sun, "Nonlinear aerostatic and aerodynamic analysis of long-span suspension bridges considering wind-structure interactions," *Journal of Wind Engineering & Industrial Aerodynamics*, vol. 90, no. 9, pp. 1065–1080, 2002.

[9] J. Cheng, J.-J. Jiang, and R.-C. Xiao, "Aerostatic stability analysis of suspension bridges under parametric uncertainty," *Engineering Structures*, vol. 25, no. 13, pp. 1675–1684, 2003.

[10] Y. Li, D. Wang, C. Wu, and X. Chen, "Aerostatic and buffeting response characteristics of catwalk in a long-span suspension bridge," *Wind and Structures, An International Journal*, vol. 19, no. 6, pp. 665–686, 2014.

[11] M. Xu, W. Guo, H. Xia, and K. Li, "Nonlinear aerostatic stability analysis of Hutong cable-stayed rail-cum-road bridge," *Wind and Structures, An International Journal*, vol. 23, no. 6, pp. 485–503, 2016.

[12] X.-J. Zhang and M. Yao, "Numerical investigation on the wind stability of super long-span partially earth-anchored cable-stayed bridges," *Wind and Structures, An International Journal*, vol. 21, no. 4, pp. 407–424, 2015.

[13] J. Cheng, J.-J. Jiang, R.-C. Xiao, and H.-F. Xiang, "Nonlinear aerostatic stability analysis of Jiang Yin suspension bridge," *Engineering Structures*, vol. 24, no. 6, pp. 773–781, 2002.

[14] Y.-J. Ge, Z.-Y. Zhou, and W.-M. Zhang, *Report of section model wind tunnel test of Maanshan Yangtze River*, Tongji University, Shanghai, China, 2009.

[15] X.-L. Hu, *Flutter, buffeting and aerostatic stability analysis for long-span cable-stayed bridges*, School of Civil Engineering. Tongji University, Shanghai, China, 2006.

[16] A. Arena, W. Lacarbonara, D. T. Valentine, and P. Marzocca, "Aeroelastic behavior of long-span suspension bridges under arbitrary wind profiles," *Journal of Fluids and Structures*, vol. 50, pp. 105–119, 2014.